



CHORUS

This is the accepted manuscript made available via CHORUS. The article has been published as:

Measurement of the $D^{\{0\}} \rightarrow \omega \eta$ branching fraction with CLEO-c data

M. J. Smith, D. Cinabro, and P. Naik

Phys. Rev. D **98**, 051101 — Published 6 September 2018

DOI: [10.1103/PhysRevD.98.051101](https://doi.org/10.1103/PhysRevD.98.051101)

Measurement of $D^0 \rightarrow \omega\eta$ Branching Fraction with CLEO-c Data

M. J. Smith

Lawrence Technological University

D. Cinabro

*Wayne State University, Department of Physics and Astronomy**

P. Naik

University of Bristol

Abstract

Using CLEO-c data, we confirm the observation of $D^0 \rightarrow \omega\eta$ by BESIII. In the Dalitz Plot of $D^0 \rightarrow K_S^0\eta\pi^0$, we find a background in the $K_S^0(\rightarrow \pi^+\pi^-)\pi^0$ projection with a $m(\pi^+\pi^-\pi^0)$ equal to the $\omega(782)$ mass. In a direct search for $D^0 \rightarrow \omega\eta$ we find a clear signal and measure $\mathcal{BF}_{D^0 \rightarrow \omega\eta} = (1.78 \pm 0.19 \pm 0.15) \times 10^{-3}$, in good agreement with BESIII.

* david.cinabro@wayne.edu

The recent observation by BESIII of $D^0 \rightarrow \omega\eta$ [1] gave clarity to us of a mystery we noted in CLEO-c data. In the Dalitz Plot of $D^0 \rightarrow K_S^0\eta\pi^0$, we observed an anomalous peak at $0.6 \text{ (GeV}/c^2)^2$ in the $m(K_S^0\pi^0)^2$ fit projection. The BESIII observation leads us to think that this peak is due to an $\omega(782) \rightarrow \pi^+\pi^-\pi^0$ candidate whose charged pions are mis-reconstructed as a K_S^0 . This decay channel has been predicted to have a branching fraction of $\mathcal{BF} = (3.3 \pm 0.2) \times 10^{-3}$ in [2], $\mathcal{BF} = (1.7 - 4.5) \times 10^{-3}$ in [3], and more recently $\mathcal{BF} = (1.0 - 3.0) \times 10^{-3}$ in [4] and [5]. Charge conjugation is implied throughout. Since the decay can proceed from both a D^0 and a \bar{D}^0 and we do no additional reconstruction to find the D flavor, we are actually measuring the average of the branching fractions of $D^0 \rightarrow \omega\eta$ and $\bar{D}^0 \rightarrow \omega\eta$.

The CLEO-c detector and its experimental methods have been described in detail elsewhere [6]. This analysis was performed on 818 pb^{-1} of $e^+e^- \rightarrow \psi(3770)$ data with center-of-mass energy $E_{\text{cm}} = 3.774 \text{ GeV}$. All D^0/\bar{D}^0 candidates are reconstructed from π^\pm , π^0 , and η that pass standard selection criteria described elsewhere [7]. Charged tracks must be well reconstructed and pass basic track quality selections. We require a track momentum between $0.050 \text{ GeV}/c \leq p \leq 2 \text{ GeV}/c$ and the tracks consistent with coming from the interaction region. We use the specific ionization, dE/dx , from the drift chambers and the Ring Imaging CHerenkov (RICH) detector to identify our selected tracks as π^\pm . If dE/dx is valid, we require a three standard deviation consistency with the π^\pm hypothesis. For tracks with $p \geq 0.70 \text{ GeV}/c$ and $|\cos\theta| < 0.8$ we can use RICH information as well. If both RICH and dE/dx are valid, we require the combined log-likelihood $\mathcal{L}_{\pi K} \leq 0$ where

$$\mathcal{L}_{\pi K} = \sigma_\pi^2 - \sigma_K^2 + L_\pi - L_K \quad (1)$$

where σ_h is the number of standard deviations the track's momentum-dependent dE/dx is from the hypothesis, and L_h is the log-likelihood of the hypothesis from the RICH information.

We reconstruct π^0 and η candidates as neutral $\rightarrow \gamma\gamma$. The unconstrained mass is calculated under the assumption that the photons originate from the interaction point. We require this mass to be within three standard deviations of the nominal π^0/η mass. A subsequent kinematic fit must not be obviously bad by removing those the fit χ^2 larger than 10000. We reject neutral candidates with both photons detected in the endcap of our calorimeter and explicitly reject any photon showers with a matched track. Aside from mass values the

selections are identical for π^0 and η candidates.

We reconstruct D^0 candidates from $\pi^+\pi^-\pi^0\eta$ combinations. We make an initial requirement that the invariant mass $m(\pi^+\pi^-\pi^0\eta)$ be within $0.100 \text{ GeV}/c^2$ of the Particle Data Group PDG [8] average D^0 mass. We select $\omega(782)$ candidates with the $\pi^+\pi^-\pi^0$ invariant mass, m_ω . We use m_ω , the beam-constrained mass of $\omega\eta$ ($M_{bc}^2 c^4 \equiv E_{Beam}^2 - p^2 c^2$ with p being their summed momentum), and ΔE , $E_{\pi^+\pi^-\pi^0\eta} - E_{Beam}$ with $E_{\pi^+\pi^-\pi^0\eta}$ being the sum of the candidate particle energies and E_{Beam} being the beam energy, to select candidates. We iterate making selections on two of the three, fitting a Gaussian signal plus smooth backgrounds in the third, making a selection based on the fit results, and repeating until the selection values do not change. In M_{bc} we fit the background to an Argus function [9], and use a 4th order polynomial in ΔE and m_ω . Unlike for M_{bc} there is no physics motivated background shape for ΔE and m_ω , and we chose a 4th order polynomial to give a reasonable model of background without adding meaningless nuisance parameters. We use the signal mean and standard deviation from one fit to make three standard deviation selections on the other plots. We generate 50000 simulated signal D^0/\bar{D}^0 events to measure the efficiency of our reconstruction and to determine the optimal widths to use in fitting to the data. We take the yield from M_{bc} and ΔE as our measurements of the D^0 yield in the simulation. From the value of M_{bc} yield, we find an efficiency of $(17.49 \pm 0.22)\%$.

The same process is performed in data, but with the widths obtained in signal simulation fixed in fits to the data distributions. We choose $\omega(782)$ candidates which have $0.760 \text{ GeV}/c^2 \leq m(\pi^+\pi^-\pi^0) \leq 0.804 \text{ GeV}/c^2$. The $m(\pi^+\pi^-\pi^0)$ mass fit is used to select $\omega(782)$ candidates, but not for measurement of the D^0 yield. The ΔE distribution is shown in Figure 1. We set this selection to $-0.0355 \text{ GeV} \leq \Delta E \leq 0.0315 \text{ GeV}$. Variations in the range of the fit displayed in Figure 1 have a negligible effect, small compared to the statistical uncertainty, on both the selection choice and signal yield. The beam-constrained mass distribution and fit is shown in Figure 2, and we select $1.859 \text{ GeV}/c^2 \leq M_{bc} \leq 1.872 \text{ GeV}/c^2$. The M_{bc} and ΔE fit yields can both be used as measurements of the $D^0 \rightarrow \omega\eta$ yield. Raw signal yields are 711 ± 65 from the M_{bc} fit and 720 ± 70 from the ΔE fit. We show the $m(\pi^+\pi^-\pi^0)$ invariant mass distribution after the selections on M_{bc} and ΔE in Figure 3, noting that there is a clear $\omega(782)$ signal.

Above, we assume the $\omega(782)$ is strongly related to the reconstruction of the D^0 and its M_{bc} . In a two dimensional plot of $\omega(782)$ mass versus M_{bc} with a three standard deviation

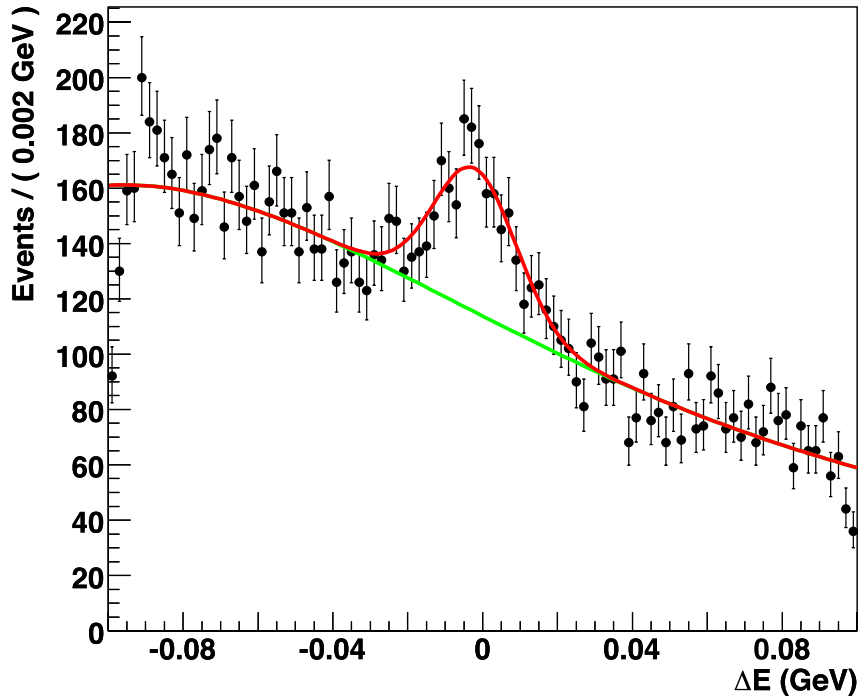


FIG. 1. The ΔE distribution and fit described in text after three standard deviation signal selections for the $\omega(782)$ and on M_{bc} .

ΔE selection we clearly see a well-populated region near the intersection of the D^0 and the $\omega(782)$ masses rising above a large background. We also find no D^0 signal in M_{bc} sidebands above and below the $\omega(782)$ mass selections.

We expect there to be some K_S^0 contamination in our $\omega(782)$ signal; after all we began with an $\omega(782)$ background in a $K_S^0\eta\pi^0$ Dalitz plot. For our signal candidates, we show the $m(\pi^+\pi^-)$ distribution in Figure 4. There is a clear K_S^0 peak. We fit this distribution using a Gaussian peak plus a 4th order polynomial background. The fit changes negligibly if we vary the bin width. There are 158 ± 20 K_S^0 events in the Gaussian peak. Not all of these should be subtracted as when we examine the M_{bc} distribution for those events within three standard deviations of the K_S^0 mean and sidebands above and below, we see signal-like peaks in the side-bands. That is some of these K_S^0 are in combinatoric backgrounds to the signal. To estimate the amount of K_S^0 contamination in our signal we fit the three M_{bc} distributions using the same method described above, and find signal and background yields

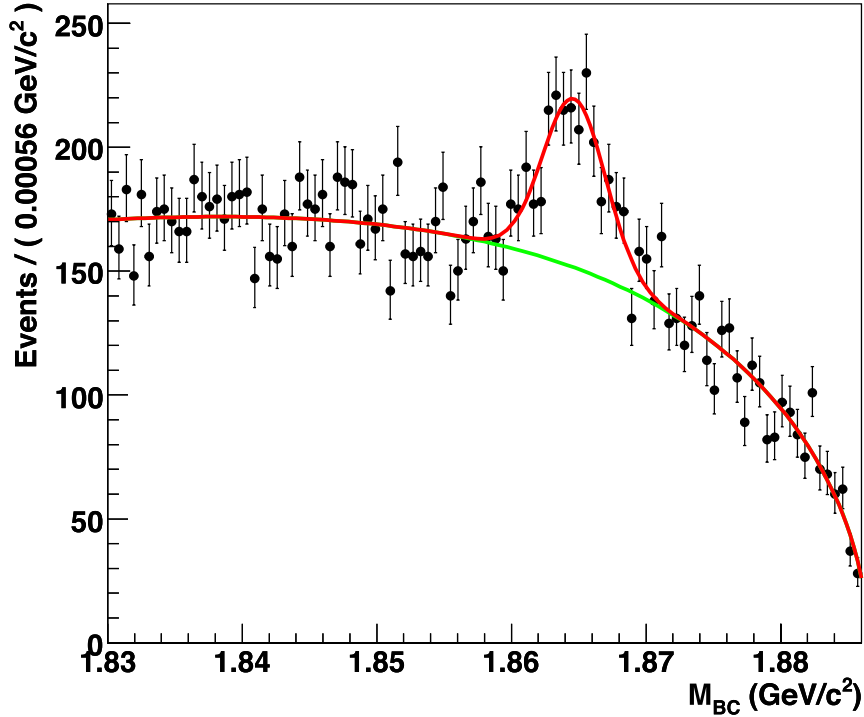


FIG. 2. The M_{bc} distribution and fit described in text after the three standard deviation signal selections on $\omega(782)$ and ΔE .

summarized in Table I. Using the signal fraction in the central M_{bc} region, we subtract

TABLE I. Signal and background yields from fitting the M_{bc} distribution in three $m(\pi^+\pi^-)$ regions around the K_S^0 peak as described in the text.

| | Below | Central | Above |
|------------|-------|---------|-------|
| Signal | 347 | 122 | 229 |
| Background | 1749 | 327 | 1649 |
| Sig/Total | 16.6% | 27.2% | 12.2% |

$(158 \pm 20) \times 27\% = 43 \pm 5$ from the observed yields. Further we include a ± 16 , 10%, uncertainty on this subtraction due to our inability to know precisely how many of the K_S^0 are from signal candidates or from background combinatorics.

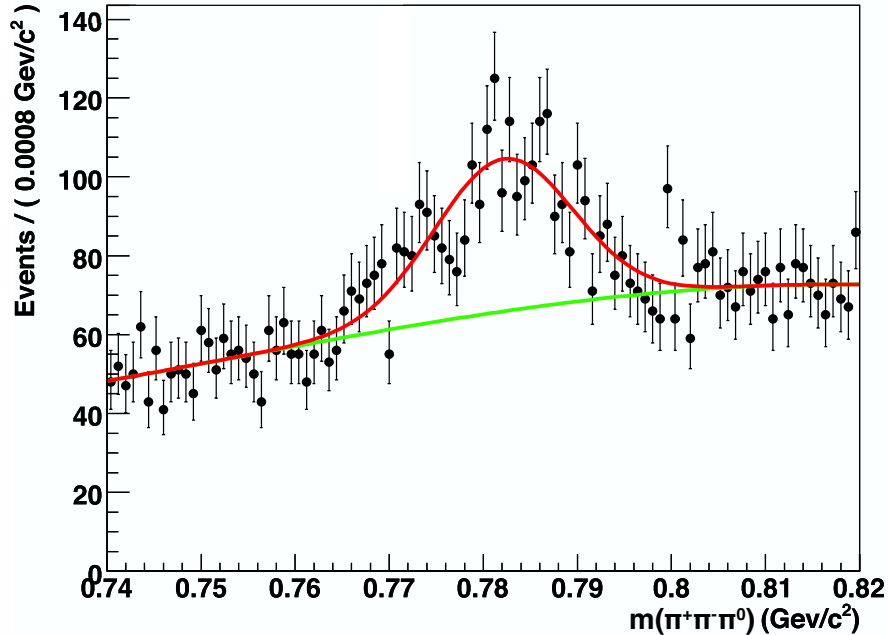


FIG. 3. The $m(\pi^+\pi^-\pi^0)$ invariant mass distribution after signal selections in ΔE and M_{bc} . The displayed fit is used to determine ω candidate selection as described in the text.

In a second method of accounting for K_S^0 contamination we veto the $K_S^0\pi^0$ contribution to $\omega(782)$ by removing the K_S^0 region in $m(\pi^+\pi^-)$. Aside from the veto, the analysis is identical to that described above. We determine a new efficiency in fits to the veto M_{bc} distribution of $(16.13 \pm 0.208)\%$ which represents an 7.8% reduction with respect to the efficiency without the K_S^0 veto.

Repeating the data analysis with the K_S^0 veto, Table II contains the K_S^0 veto analysis yields. Table III contains the yields from ΔE and M_{bc} corrected by both K_S^0 subtraction and veto, as well as their associated efficiencies and efficiency corrected yields.

The analyses described above used signal widths observed in the signal simulation fixed in the data fits. When we float these widths in the K_S^0 veto analysis, we find 637 ± 89 and 521 ± 85 for the M_{bc} and ΔE signal yields, respectively. These values greatly differ from those with fixed widths, and indeed greatly from each other. We will use the difference between fixed and floating M_{bc} yields as a systematic uncertainty.

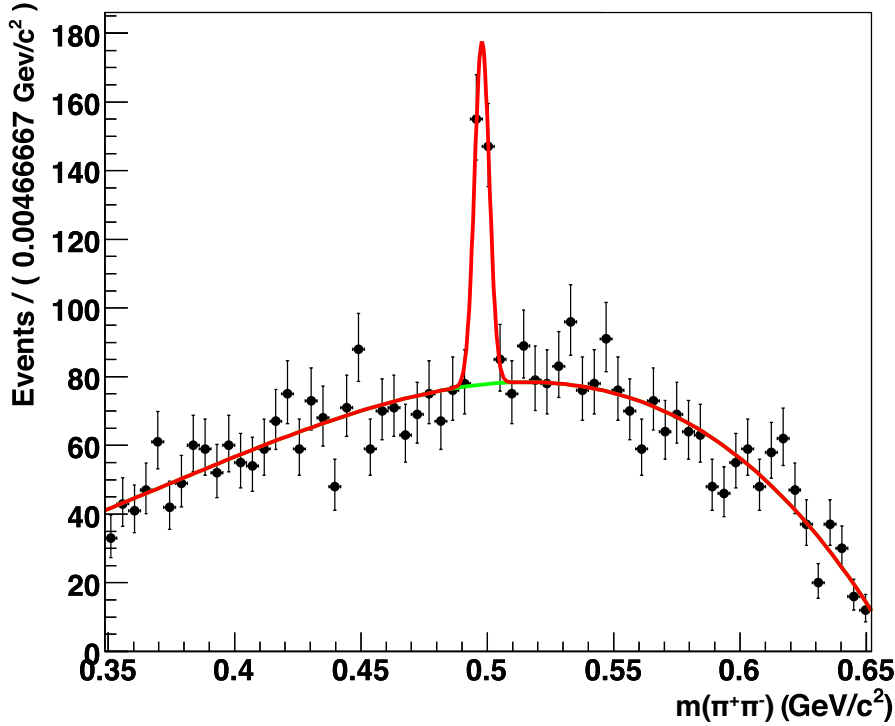


FIG. 4. The $m(\pi^+\pi^-)$ distribution for signal candidates. The fit is described in the text.

TABLE II. Summary of Signal Selections with K_S^0 Veto

| Signal Selections |
|------------------------------------------------------------------------------------------|
| $m(\pi^+\pi^-) \leq 0.489 \text{ GeV}/c^2$ or $m(\pi^+\pi^-) \geq 0.507 \text{ GeV}/c^2$ |
| $0.760 \text{ GeV}/c^2 \leq m(\pi^+\pi^-\pi^0) \leq 0.805 \text{ GeV}/c^2$ |
| $-0.0355 \text{ GeV} \leq \Delta E \leq 0.0315 \text{ GeV}$ |
| $1.859 \text{ GeV}/c^2 \leq M_{bc} \leq 1.872 \text{ GeV}/c^2$ |

We calculate the branching fraction using

$$\mathcal{BF}_{D^0 \rightarrow \omega\eta} = \frac{N_{D^0 \rightarrow \omega\eta}}{2\epsilon_{D^0 \rightarrow \omega\eta} N_{D^0 \bar{D}^0} \mathcal{BF}_{\omega \rightarrow \pi^+\pi^-\pi^0} \mathcal{BF}_{\eta \rightarrow \gamma\gamma} \mathcal{BF}_{\pi^0 \rightarrow \gamma\gamma}} \quad (2)$$

where $N_{D^0 \rightarrow \omega\eta}$ is the observed yield, ϵ is the appropriate efficiency, and $N_{D^0 \bar{D}^0}$ is the total number of D^0/\bar{D}^0 events. We calculate $N_{D^0 \bar{D}^0}$ by multiplying the cross section for $e^+e^- \rightarrow D^0 \bar{D}^0$ previously reported by CLEO [7] and our integrated luminosity. Table IV contains

TABLE III. Signal Yields from Fittings Accounting for K_S^0 Effects

| | Type | Yield | Efficiency | Yield/Efficiency |
|---------------------------|------------|--------------|----------------------|------------------|
| K_S^0 Events Subtracted | M_{bc} | 667 ± 67 | $(17.49 \pm 0.22)\%$ | 3819 |
| | ΔE | 677 ± 72 | $(17.06 \pm 0.22)\%$ | 3969 |
| K_S^0 Veto | M_{bc} | 596 ± 62 | $(16.13 \pm 0.21)\%$ | 3694 |
| | ΔE | 597 ± 67 | $(15.79 \pm 0.21)\%$ | 3780 |

the branching fraction inputs.

Comparing the yield divided by efficiency results in Table III we see the K_S^0 Subtraction and Veto are both acceptable methods to deal with K_S^0 contamination giving consistent results. The four efficiency corrected yields have a standard deviation of 115, which is 3.0% of the average efficiency corrected yield of 3816. The efficiency corrected yields are larger in the subtraction method and this method has a conceptual problem. Our subtraction choice is a best guess; there is no clear way to determine how many K_S^0 actually contaminate the signal rather than coming from the background.

We therefore take the M_{bc} yield from the K_S^0 veto analysis as the best measurement. Comparing using M_{bc} and ΔE to extract the yield, we have a fortunately small ± 1 systematic uncertainty from the difference in signal yield and $\pm 0.34\%$ uncertainty from the difference in efficiency. These give a 2.13% relative uncertainty on the efficiency corrected yield. We also have a ± 41 systematic due to the difference between using fixed and floating widths in M_{bc} fits. These two yield uncertainties give us a total systematic uncertainty on the yield. We find $\mathcal{BF}_{D^0 \rightarrow \omega\eta} = (1.78 \pm 0.19 \pm 0.15) \times 10^{-3}$. The statistical uncertainty comes from the statistical uncertainty in the signal yield. We also include relative 0.7% and 2.0% uncertainty on charged and neutral particle reconstruction efficiencies derived from our simulation added in quadrature for an additional 3.0% relative uncertainty on our efficiency [10]. All of the uncertainties are summarized in Table V. The contribution from $\mathcal{BF}(\pi^0 \rightarrow \gamma\gamma)$ is negligible.

In summary, in the CLEO-c data we have observed $D^0 \rightarrow \omega\eta$ and measure the average branching fraction of $D^0 \rightarrow \omega\eta$ and $\bar{D}^0 \rightarrow \omega\eta$ as

$$\mathcal{BF}(D^0 \rightarrow \omega\eta) = (1.78 \pm 0.19 \pm 0.15) \times 10^{-3}, \quad (3)$$

TABLE IV. Summary of Branching Fraction Inputs. Branching Fractions are PDG [8] values. Uncertainties are statistical and systematic, respectively.

| Quantity | Value |
|---------------------------------------------------------|-------------------------------------|
| Signal Yield | $596 \pm 62 \pm 1$ |
| MC Efficiency | $(16.13 \pm 0.21 \pm 0.59)\%$ |
| Reconstruction Uncertainties | $\pm 3.0\%$ |
| $\mathcal{BF}(\omega(782) \rightarrow \pi^+\pi^-\pi^0)$ | $(89.2 \pm 0.7)\%$ |
| $\mathcal{BF}(\eta \rightarrow \gamma\gamma)$ | $(39.31 \pm 0.20)\%$ |
| $\mathcal{BF}(\pi^0 \rightarrow \gamma\gamma)$ | $(98.823 \pm 0.034)\%$ |
| $\sigma(e^+e^- \rightarrow D^0\bar{D}^0)$ | $(3.66 \pm 0.03 \pm 0.06)\text{nb}$ |
| Luminosity | $818 \pm 8 \text{ pb}^{-1}$ |
| $N_{D^0\bar{D}^0}$ | 2993880 |

where the first uncertainty is statistical and the second systematic. This agrees with the previous observation by BESIII [1]. Our measured branching fraction is at the lower side of the range given by the most recent theory predictions [4, 5]. We note that this D^0 decay mode is a CP-eigenstate making it a potentially valuable tool in heavy flavor analysis.

This investigation was done using CLEO data, and as members of the former CLEO Collaboration we thank it for this privilege. This research was supported by the U.S. National Science Foundation.

TABLE V. Summary of the uncertainties on $\mathcal{BF}_{D^0 \rightarrow \omega \eta}$.

| Source | Value ($\times 10^{-3}$) |
|-----------------------------------------------------------|----------------------------|
| Statistical on Yield | ± 0.19 |
| Signal Yield | ± 0.125 |
| MC Efficiency | ± 0.060 |
| Reconstruction Efficiency | ± 0.053 |
| Luminosity | ± 0.0178 |
| Cross Section | ± 0.0326 |
| $\mathcal{BF}(\omega(782) \rightarrow \pi^+ \pi^- \pi^0)$ | ± 0.0140 |
| $\mathcal{BF}(\eta \rightarrow \gamma\gamma)$ | ± 0.00906 |
| Total Systematic | ± 0.154 |
| Total Uncertainty | ± 0.24 |

-
- [1] M. Ablikim *et al.* (BESIII Collaboration), Phys. Rev. D **97**, 052005 (2018).
- [2] B. Bhattacharya and J. L. Rosner, Phys. Rev. D, **82** 037502 (2010).
- [3] Hai-Yang Cheng and Cheng-Wei Chiang Phys. Rev. D **81**, 074021 (2010).
- [4] Qin Qin, Hsiang-nan Li, Cai-Dian L, and Fu-Sheng Yu Phys. Rev. D **89**, 054006 (2014).
- [5] Hai-Yang Cheng, Cheng-Wei Chiang, and An-Li Kuo Phys. Rev. D **93**, 114010 (2016).
- [6] Y. Kubota *et al.* (CLEO Collaboration), Nucl. Instrum. Methods Phys. Res., Sect. A **320**, 66 (1992); D. Peterson *et al.*, Nucl. Instrum. Methods Phys. Res., Sect. A **478**, 142 (2002); M. Artuso *et al.*, Nucl. Instrum. Methods Phys. Res., Sect. A **554**, 147 (2005); CLEO-c/CESR-c Taskforces & CLEO-c Collaboration, Cornell LEPP Report No. CLNS 01/1742 (2001) (unpublished).
- [7] G. Bonvicini *et al.* (CLEO Collaboration), Phys. Rev. D **89**, 072002 (2014).
- [8] C. Patrignani *et al.* (Particle Data Group), Chin. Phys. C, **40**, 100001 (2016) and 2017 update.
- [9] H. Albrecht *et al.* (ARGUS Collaboration) (1990) Physics Letters B. 241 (2): 278282 (1990).
- [10] Q. He *et al.* (CLEO Collaboration), Phys. Rev. Lett. **95**, 121801 (2015); erratum-ibid. **96** 199903 (2006).